

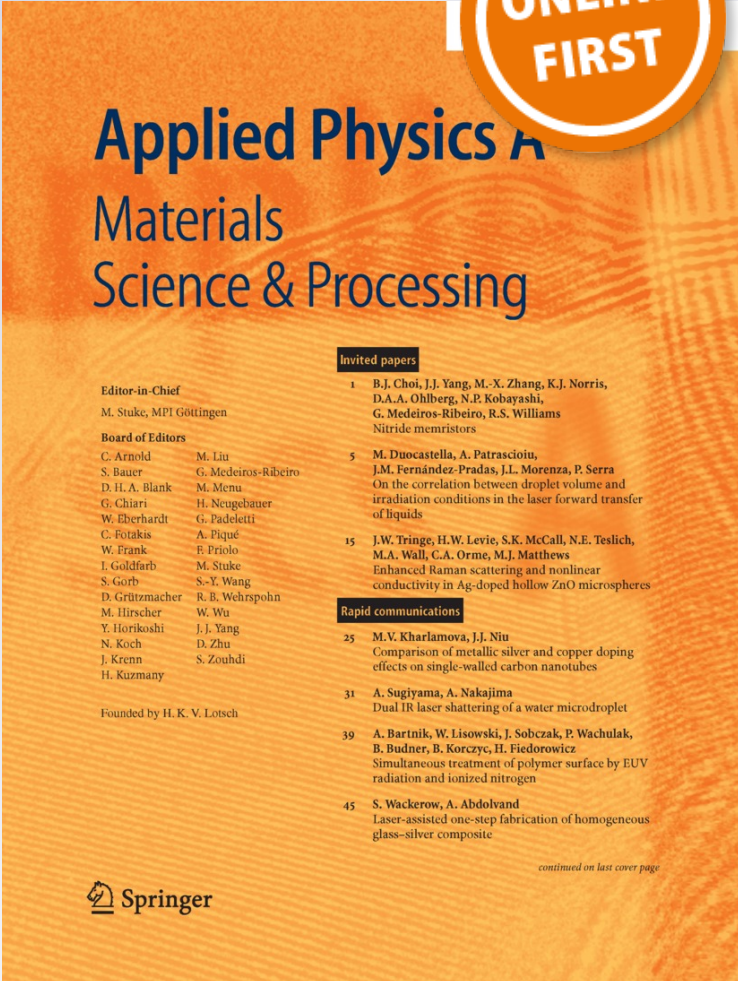
On the magnetic compensation of magnesium doped Ni-Cr ferrites

**A. Rais, A. Addou, M. Ameri,
N. Bouhadouza & A. Merine**

Applied Physics A
Materials Science & Processing

ISSN 0947-8396

Appl. Phys. A
DOI 10.1007/s00339-012-7304-9



Applied Physics A
Materials
Science & Processing

**ONLINE
FIRST**

Invited papers

- 1 B.J. Choi, J.J. Yang, M.-X. Zhang, K.J. Norris, D.A.A. Ohlberg, N.P. Kobayashi, G. Medeiros-Ribeiro, R.S. Williams
Nitride memristors
- 5 M. Duocastella, A. Patrascioiu, J.M. Fernández-Pradas, J.L. Morenza, P. Serra
On the correlation between droplet volume and irradiation conditions in the laser forward transfer of liquids
- 15 J.W. Tringe, H.W. Levie, S.K. McCall, N.E. Teslich, M.A. Wall, C.A. Orme, M.J. Matthews
Enhanced Raman scattering and nonlinear conductivity in Ag-doped hollow ZnO microspheres

Rapid communications

- 25 M.V. Kharlamova, J.J. Niu
Comparison of metallic silver and copper doping effects on single-walled carbon nanotubes
- 31 A. Sugiyama, A. Nakajima
Dual IR laser shattering of a water microdroplet
- 39 A. Bartnik, W. Lisowski, J. Sobczak, P. Wachulak, B. Budner, B. Korczyk, H. Fiedorowicz
Simultaneous treatment of polymer surface by EUV radiation and ionized nitrogen
- 45 S. Wackerow, A. Abdolvand
Laser-assisted one-step fabrication of homogeneous glass-silver composite

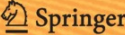
continued on last cover page

Editor-in-Chief
M. Stuke, MPI Göttingen

Board of Editors

C. Arnold	M. Liu
S. Bauer	G. Medeiros-Ribeiro
D. H. A. Blank	M. Menu
G. Chiari	H. Neugebauer
W. Eberhardt	G. Padeletti
C. Fotakis	A. Piqué
W. Frank	F. Priolo
I. Goldfarb	M. Stuke
S. Görb	S.-Y. Wang
D. Grützmacher	R. B. Wehrspohn
M. Hirscher	W. Wu
Y. Horikoshi	J. J. Yang
N. Koch	D. Zhu
J. Krenn	S. Zoubdi
H. Kuzmany	

Founded by H. K. V. Lotsch

 Springer

Your article is protected by copyright and all rights are held exclusively by Springer-Verlag Berlin Heidelberg. This e-offprint is for personal use only and shall not be self-archived in electronic repositories. If you wish to self-archive your work, please use the accepted author's version for posting to your own website or your institution's repository. You may further deposit the accepted author's version on a funder's repository at a funder's request, provided it is not made publicly available until 12 months after publication.

On the magnetic compensation of magnesium doped Ni-Cr ferrites

A. Rais · A. Addou · M. Ameri · N. Bouhadouza ·
A. Merine

Received: 31 July 2012 / Accepted: 26 September 2012
© Springer-Verlag Berlin Heidelberg 2012

Abstract Mg-substituted ferrites $\text{NiMg}_x\text{Fe}_{1.1-(2/3)x}\text{Cr}_{0.9}\text{O}_4$ ($0 \leq x \leq 0.4$) were studied using X-ray diffraction, Mössbauer spectroscopy, and magnetic measurements. X-ray diffraction patterns show that all samples have cubic spinel structure. The temperature-dependent magnetic measurements revealed that the compensation point T_K of $\text{NiFe}_{1.1}\text{Cr}_{0.9}\text{O}_4$ starts to approach the Curie temperature T_C as Mg^{2+} substitution of Fe^{3+} increases, until the magnetic compensation disappears at composition $x = 0.4$. The magnetization data at all concentrations are discussed in the light of Néel's molecular field model given the cations distribution obtained using the Mössbauer spectra analysis.

1 Introduction

In the classical theory of ferrimagnets, Néel predicted the existence of a magnetic compensation temperature in 1948 [1], but the first experimental observation was reported only in 1953 in certain metal oxides [2], and more recently in molecular magnets [3]. McGuire and Greenwald [4] were the first to observe the magnetic compensation effect in chromium-doped nickel ferrites $\text{NiFe}_{2-x}\text{Cr}_x\text{O}_4$ at $x = 1.3$ and unlike other ferrites exhibiting this phenomenon [5], the main difficulty encountered in the interpretation of this

system is due to the presence of three kinds of magnetically active Ni^{2+} , Fe^{3+} , and Cr^{3+} ions. In a previous paper [6], we agreed with Miyahara and Tsushima [7] that the $\text{NiFe}_{2-x}\text{Cr}_x\text{O}_4$ ferrites of $x \leq 1$ have a completely inverted spinel structure unlike Ni-Zn ferrites [8]. Others, like Mg-Zn ferrites [9] change from normal to inverse spinel as one cation (Zn^{2+}) is replaced by another (Mg^{2+}). Furthermore, we have found that given the cation distribution of this system obtained by Mössbauer spectroscopy, its magnetic properties are interpreted reasonably well by Neel's molecular field model of ferrimagnetism.

In this work, we report the effect of Mg^{2+} substitution for Fe^{3+} on the magnetic compensation of nickel-chromium ferrites. Moreover, using a Mössbauer study of this system, we propose a cation distribution for $\text{NiMg}_x\text{Fe}_{1.1-(2/3)x}\text{Cr}_{0.9}\text{O}_4$ ($0 \leq x \leq 0.4$), and investigate its relationship with the magnetic compensation effect.

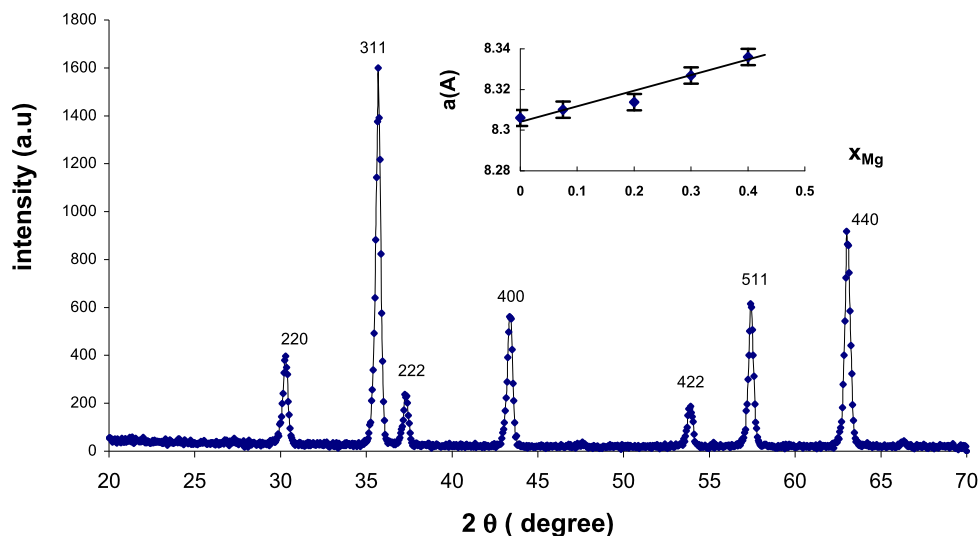
2 Experimental

Five samples of the ferrite system $\text{NiMg}_x\text{Cr}_{0.9}\text{Fe}_{1.1-(2/3)x}\text{O}_4$ ($0 \leq x \leq 0.4$) were prepared by the conventional double-sintering ceramic technique. The starting materials were analytical reagent grade NiCO_3 , Fe_2O_3 , MgO , and Cr_2O_3 (BDH), and were weighed stoichiometrically as per chemical formula unit. The samples were ground into fine powder for one hour in an agate mortar then compressed using an unidirectional hydraulic press at 4 tons/cm² to form pellets. The dried pellets were presintered in air at 1000 °C for 12 hours. The final sintering was at 1200 °C for 12 hours then slowly furnace cooled to room temperature at a rate of 20 °C/min. Powdered specimens were prepared for the X-ray diffraction, Mössbauer spectroscopy, and magnetization measurements.

A. Rais (✉) · M. Ameri · N. Bouhadouza · A. Merine
Département de Physique, Faculté des Sciences, Université Djilali
Liabes, Sidi Bel Abbès, Algeria
e-mail: amrais@yahoo.com

A. Addou
Laboratoire STEVA, Département de Chimie, Université
de Mostaganem, Mostaganem, Algeria

Fig. 1 X-ray representative spectrum of $\text{NiFe}_{1.1}\text{Cr}_{0.9}\text{O}_4$. The inset shows the lattice parameter a (Angstroms) versus the magnesium content of $\text{NiMg}_x\text{Cr}_{0.9}\text{Fe}_{1.1-(2/3)x}\text{O}_4$



The X-ray data were collected using a Philips PW1820 vertical goniometer with monochromator and automatic divergence slit attached to a $\text{CuK}\alpha$ PW1700 generator operating at a voltage of 40 kV, current 40 mA and controlled by a PDP11 computer. Scans in the $2\theta = 20^\circ$ – 70° range were obtained using a step size of 0.02° and sample time of 2 s. The peak positions were identified using the Philips APD peak search program and the JCPDS files enabled the indexing.

Liquid nitrogen and room temperature Mössbauer spectra were obtained using a $^{57}\text{CoRh}$ source and a spectrometer in the constant acceleration mode. Least square fitting techniques were used for the analysis of the data and α -Fe for the calibration of the spectrometer.

The magnetization measurements were performed using a vibrating sample magnetometer (VSM) of 10^{-5} emu sensitivity. The magnetic field ranged from 0 to 13.5 kOe and the temperatures (T) were scanned within a range of 77 K to 650 K. The VSM system has an incorporated cryostat/oven device that is utilized for both low and high T measurements without removing the sample. The VSM was calibrated using a 99.99 % pure nickel sample with a standard magnetization value of $M_S = 54.9$ emu/g.

3 Results and discussion

X-ray diffraction analysis showed the formation of cubic spinel structure for all five samples. A representative diffraction of $\text{NiCr}_{0.9}\text{Fe}_{1.1}\text{O}_4$ is shown in Fig. 1. First, the lattice parameters were calculated for different planes as shown in Fig. 1 at the different diffraction angle 2θ . Then the lattice parameter (a) was obtained from the extrapolation to $\theta = 90^\circ$ of the graph a against the error function $1/2(\cos^2\theta/\sin\theta + \cos 2\theta/\theta)$. The overall error was estimated at 0.001 \AA . The results are in good agreement with

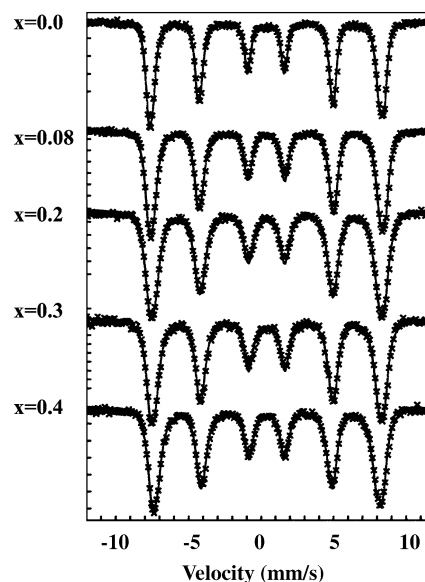


Fig. 2 Mössbauer spectra of $\text{NiMg}_x\text{Cr}_{0.9}\text{Fe}_{1.1-(2/3)x}\text{O}_4$ at 77 K

Lee et al. [10] for $x = 0$. As can be seen in the inset of Fig. 1, within the error bars, the lattice parameter increases slowly with the magnesium content. This variation reflects the larger radius of Mg^{2+} as compared to Fe^{3+} .

Figure 2 shows ^{57}Fe Mössbauer spectra of ferrites $\text{NiCr}_x\text{Fe}_{2-x}\text{O}_4$ ($0 \leq x \leq 1.4$) recorded at 77 K. The room temperature spectra shows patterns similar to 77 K, but with more broadened outer lines. In fitting the spectra, we adopted a simple model using two overlapping sextets for the tetrahedral (A) and octahedral [B] coordination sites for iron. The spectra were least square fitted to Lorentzian line-shapes using MOSFIT. The fitted subspectra are shown as full lines in Fig. 2. All the hyperfine interaction parameters, given in Table 1, were allowed to vary freely in the fitting process. The linewidth of the outer absorption line

Table 1 Mössbauer parameters of $\text{NiMg}_x\text{Cr}_{0.9}\text{Fe}_{1.1-(2/3)x}\text{O}_4$ at 77 K

x	Tetrahedral A-site				Octahedral B-site			
	IS mm/s	LW mm/s	H(T)	A%	IS mm/s	LW mm/s	H(T)	A%
0.0	0.34	0.55	49.9	92	0.47	0.55	53.1	8
0.08	0.37	0.54	50.8	84	0.43	0.51	52.8	16
0.2	0.36	0.56	50.3	80	0.40	0.48	52.1	20
0.3	0.36	0.59	49.6	73	0.38	0.45	51.3	27
0.4	0.34	0.65	47.8	45	0.38	0.65	50.4	58

Table 2 Cation distribution of $\text{NiMg}_x\text{Cr}_{0.9}\text{Fe}_{1.1-(2/3)x}\text{O}_4$ obtained from Mössbauer analysis. Round brackets denote A sites. Square brackets denote B sites. Theoretical and experimental magnetic mo-

ments $M(\mu_B)$ per formula unit at 0 K. M_A and M_B are the magnetic moments of A and B sublattices, respectively. $M_0 = M_B - M_A$ is the net theoretical moment of the whole lattice

x	Cation distribution	$M(\mu_B)$			Experiment
		Theory			
		M_A	M_B	M_0	
0	(Fe) [NiCr _{0.9} Fe _{0.1}]	5	5.2	0.2	0.6
0.08	(Fe _{0.92} Mg _{0.08}) [NiCr _{0.9} Fe _{0.125}]	4.63	5.33	0.7	0.9
0.2	(Fe _{0.8} Mg _{0.2}) [NiCr _{0.9} Fe _{0.167}]	4	5.54	1.54	1.7
0.3	(Fe _{0.7} Mg _{0.3}) [NiCr _{0.9} Fe _{0.2}]	3.5	5.7	2.2	2.4
0.4	(Fe _{0.6} Mg _{0.4}) [NiCr _{0.9} Fe _{0.233}]	3	5.87	2.87	3.3

of each spectrum shows a broadening, and increases with the magnesium content. This could give an estimation of the distribution of the hyperfine fields at each site.

Taking the fitted absorption areas as proportional to iron site occupancies, Table 2 shows the proposed cation distributions. It is well known from previous studies that Mg^{2+} occupies A-sites [11] and Cr^{3+} occupies B-sites [12]. On the other hand, from earlier reports, nickel-chromium ferrites [6, 13] have been interpreted with Ni^{2+} occupying preferentially the octahedral sites. The rest of the tetrahedral and octahedral sites have been filled with Fe^{3+} cations in accordance with our Mössbauer absorption areas results.

On the basis of Neel's molecular field model [1] and the cation distributions given in Table 2, the magnetic moment in ferrites is mainly from the parallel-uncompensated electron spin of the individual ions, and the spin alignments in the two sublattices are arranged antiparallel. Also, the A–B exchange interaction is predominant over the A–A and B–B interactions. Hence, the net magnetic moment of the lattice is given by the algebraic sum of the magnetic moments of A and B sublattices, i.e., $M_0 = M_B - M_A$. Given the electronic configurations of the B- and A-site cations [Fe^{3+} ($3d^5$), Cr^{3+} ($3d^3$) and Ni^{2+} ($3d^8$)], we can estimate the sublattice magnetizations using the spin-only values of Fe^{3+} ($5\mu_B$), Cr^{3+} ($3\mu_B$) and Ni^{2+} ($2\mu_B$) assuming a weak spin-orbit coupling. The calculated spin magnetic moments M_0 at 0 K are shown in Table 2 and appear to increase with the magnesium content.

Measured saturation magnetization M_S of all compositions against temperature are shown in Fig. 3. At $x = 0$, M_S values are in good agreement with those of Belov et al. [14] as well as the compensation temperature T_K (360 K) and the Curie temperature T_C (580 K).

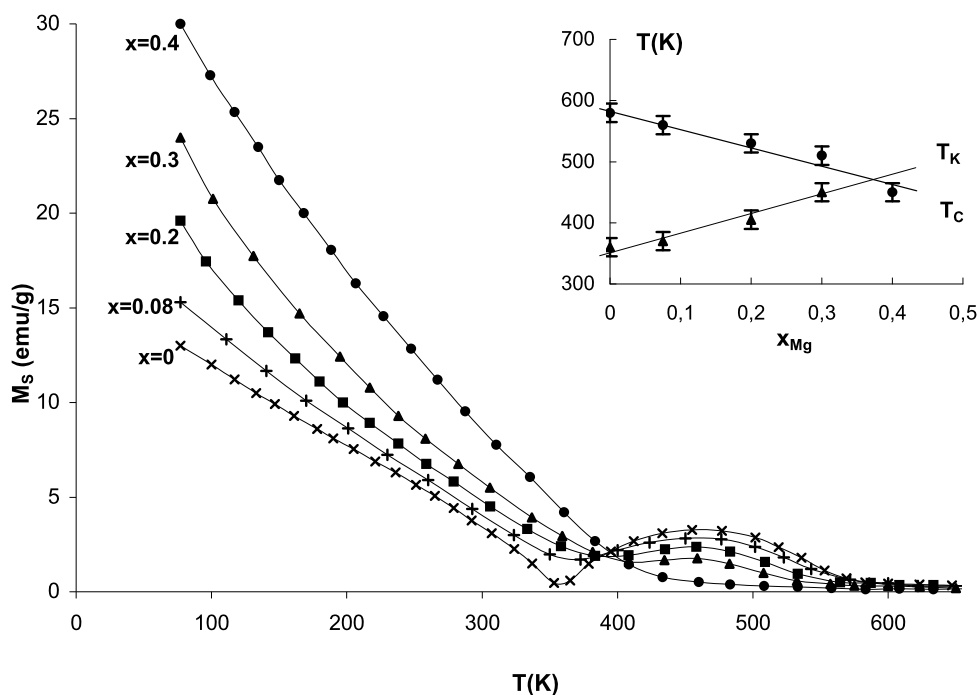
The inset in Fig. 3 shows T_C and T_K against magnesium concentration x . The Curie temperatures T_C were obtained from magnetizations versus temperature using the standard method of the “intersecting tangents” [15]. This method consists of drawing two tangents to the curve on either side where the magnetic-paramagnetic transition appears to occur. The intersection of the two tangents is at T_C . The error bars were estimated from the uncertainty in drawing the two tangents. T_K errors bars were estimated from the sharpness of the minima of M_S versus T curves.

The experimental magnetic moments in Bohr magnetons μ_B $M(\mu_B)$ at 0 K were obtained using the formula:

$$M(\mu_B) = \frac{\text{Molarweight} \times M_S(0)}{5586}$$

where $M_S(0)$ is the extrapolated value to $T = 0$ K of the graphical plot of M_S against Bloch's $T^{3/2}$ law. In the exact formula of Dyson [16], there are terms with T^2 and $T^{5/2}$ besides $T^{3/2}$ and the linear extrapolation does not give the true absolute value of $M_S(0)$, but it is good enough for the relative variations with the substitution rate of the sites occupancies. Theoretical and experimental results are shown in Table 2. Note that the error in $M_S(0)$ due to this linear extrapolation between 0 and 77 K can be as high as 15 %.

Fig. 3 Saturation magnetizations versus temperature of $\text{NiMg}_x\text{Cr}_{0.9}\text{Fe}_{1.1-(2/3)x}\text{O}_4$. The inset shows the Curie and compensation temperatures T_C and T_K versus the magnesium content



Nevertheless, it is interesting to point out the gradual increase of M_S with the addition of magnesium at temperatures below T_K . This trend is consistent with the calculated M_0 values (Table 2) obtained using the cation distribution deduced from our Mössbauer analysis.

As expected, the inset shows a decreasing T_C as more diamagnetic Mg^{2+} replaces Fe^{3+} . Moreover, Fig. 3 shows that M_S decreases with the magnesium content at temperatures between T_K and T_C . This is also expected since T_K gradually approaches T_C as the inset shows. Indeed, on extrapolating the compensation line, the intersection with the Curie line represents the point where compensation disappears, i.e., $x \approx 0.38$. This value is consistent with our direct observation at concentration $x = 0.4$.

This effect of the disappearance of magnetic compensation can be interpreted on the basis of Neel's molecular field model and the concept of the "weak" magnetic sublattice as introduced by Belov [14]. In the case of $\text{NiMg}_x\text{Cr}_{0.9}\text{Fe}_{1.1-(2/3)x}\text{O}_4$, we may consider A-sites as the magnetically strong sublattice because of the relatively higher content of Fe^{3+} cations and the B-sites as the weak sublattice. As diamagnetic Mg^{2+} substitutes Fe^{3+} in A-sites only, exchange interactions A–A are modified in such a way that the magnetization M_A of A sublattice becomes weaker. This means that the decrease rate of M_A with temperature becomes higher, and subsequently the compensation occurs at a point T_K gradually approaches T_C . The compensation disappears at a magnesium content as such that A sublattice has weakened enough so to disable the compensation of B sublattice over the whole temperature range up to T_C . Note

that as Mg^{2+} substitutes Fe^{3+} in A-sites, the net moment $M = M_B - M_A$ increases because M_A decreases while M_B stays almost constant. This is due to the relatively unchanged content of the magnetic cations Fe^{3+} and Cr^{3+} in B-sites.

4 Conclusion

We may conclude from the study of the effect of Mg^{2+} on the magnetic compensation of nickel-chromium ferrite that:

1. The magnetic compensation in $\text{NiFe}_{1.1}\text{Cr}_{0.9}\text{O}_4$ disappears when Fe^{3+} in A-site is partially replaced by Mg^{2+} .
2. Below the compensation temperature, the observed magnetic moment of these ferrites increases with the magnesium content.
3. The magnetic moments calculated using cations distribution consistent with the Mössbauer study of these ferrites, show an increasing trend with magnesium content. This trend agrees with the magnetic measurements.

References

1. L. Neel, Ann. Phys. **3**, 137 (1948)
2. E.W. Gorter, J.A. Schulkes, Phys. Rev. **89**, 487–488 (1953)
3. S. Ohkoshi, Y. Abe, A. Fujishima, K.H. Hashimoto, Phys. Rev. Lett. **8**(2), 1285 (1999)
4. T.S. McGuire, S.W. Greenwald, Sol. St. Phys. Electr. Tel. **3**(1), 50 (1960)
5. M.V. Kuznetsov, Q.A. Pankhurst, I.P. Parkin, J. Phys. D, Appl. Phys. **31**, 2886 (1998)

6. A. Rais, A.M. Gismelseed, I.A. Al-Omari, Phys. Status Solidi (b) **242**, 1497–1503 (2005)
7. S. Miyahara, T. Tsushima, J. Phys. Soc. Jpn. **13**, 758 (1958)
8. M.A. Amer, A. Tawfik, A.G. Mostafa, A.F. El-Shora, S.M. Zaki, J. Magn. Magn. Mater. **323**, 1445–1452 (2011)
9. K.A. Mohammed, A.D. Al-Rawas, A.M. Gismelseed, A. Sellai, H.M. Widatallah, A. Yousif, M.E. Elzain, M. Shongwe, Physica B **407**, 795–804 (2012)
10. S.H. Lee, S.J. Yoon, G.J. Lee, H.S. Kim, C.H. Yo, K. Ahn, D.H. Lee, K.H. Kim, Mater. Chem. Phys. **61**, 147–152 (1999)
11. G.A. Fatseas, J.L. Dorman, H. Blanchard, J. Phys. **12**, 787 (1976)
12. Y.L. Chen, B.B. Xu, J.G. Chen, Hyperfine Interact. **70**, 1029 (1976)
13. T.R. McGuire, S.W. Greenwald, Sol. St. Phys. Electr. Tel. **58**, 515 (1970)
14. K.P. Belov, Phys. Usp. **39**, 623 (1996)
15. D. Jiles, *Magnetism and Magnetic Materials* (Chapman and Hall, New York, 1990)
16. F.J. Dyson, Phys. Rev. **102**, 1230 (1956)